

SDWFS-MT-1: A SELF-OBSCURED LUMINOUS SUPERNOVA AT $z \simeq 0.2$

SZYMON KOZŁOWSKI¹, C. S. KOCHANEK^{1,2}, D. STERN³, J. L. PRIETO^{4,14}, K. Z. STANEK^{1,2}, T. A. THOMPSON^{1,2}, R. J. ASSEF¹, A. J. DRAKE⁵, D. M. SZCZYGIEL^{1,6}, P. R. WOŹNIAK⁷, P. NÜGENT⁸, M. L. N. ASHBY⁹, E. BESHORE¹⁰, M. J. I. BROWN¹¹, ARJUN DEY¹², R. GRIFFITH³, F. HARRISON⁵, B. T. JANNUZI¹², S. LARSON¹⁰, K. MADSEN⁵, B. PILECKI^{6,13}, G. POJMAŃSKI⁶, J. SKOWRON¹, W. T. VESTRAND⁷, AND J. A. WREN⁷

¹ Department of Astronomy, The Ohio State University, 140 West 18th Avenue, Columbus, OH 43210, USA; simkoz@astronomy.ohio-state.edu

² The Center for Cosmology and Astroparticle Physics, The Ohio State University, Columbus, OH 43210, USA

³ Jet Propulsion Laboratory, California Institute of Technology, 4800 Oak Drive, Pasadena, CA 91109, USA

⁴ Carnegie Observatories, 813 Santa Barbara Street, Pasadena, CA 91101, USA

⁵ California Institute of Technology, 1200 E. California Blvd, Pasadena, CA 91125, USA

⁶ Warsaw University Observatory, Al. Ujazdowskie 4, 00-478 Warsaw, Poland

⁷ Los Alamos National Laboratory, ISR-1, MS-D466, Los Alamos, NM 87545, USA

⁸ Lawrence Berkeley National Laboratory, 1 Cyclotron Road, Berkeley, CA 94720, USA

⁹ Harvard-Smithsonian Center for Astrophysics, 60 Garden Street, Cambridge, MA 02138, USA

¹⁰ Department of Planetary Sciences, Lunar and Planetary Laboratory, The University of Arizona, 1629 E. University Blvd, Tucson, AZ 85721, USA

¹¹ School of Physics, Monash University, Clayton 3800, Victoria, Australia

¹² National Optical Astronomical Observatory, 950 North Cherry Avenue, Tucson, AZ 85719, USA

¹³ Departamento de Física, Universidad de Concepción, Casilla 160-C, Concepción, Chile

Received 2010 June 21; accepted 2010 August 24; published 2010 October 1

ABSTRACT

We report the discovery of a 6 month long mid-infrared transient, SDWFS-MT-1 (aka SN 2007va), in the *Spitzer* Deep, Wide-Field Survey of the NOAO Deep Wide-Field Survey Boötes field. The transient, located in a $z = 0.19$ low-luminosity ($M_{[4.5]} \simeq -18.6$ mag, $L/L_\star \simeq 0.01$) metal-poor ($12 + \log(\text{O}/\text{H}) \simeq 7.8$) irregular galaxy, peaked at a mid-infrared absolute magnitude of $M_{[4.5]} \simeq -24.2$ in the $4.5 \mu\text{m}$ *Spitzer*/IRAC band and emitted a total energy of at least 10^{51} erg. The optical emission was likely fainter than the mid-infrared, although our constraints on the optical emission are poor because the transient peaked when the source was “behind” the Sun. The *Spitzer* data are consistent with emission by a modified blackbody with a temperature of ~ 1350 K. We rule out a number of scenarios for the origin of the transient such as a Galactic star, active galactic nucleus activity, γ -ray burst, tidal disruption of a star by a black hole, and gravitational lensing. The most plausible scenario is a supernova (SN) exploding inside a massive, optically thick circumstellar medium, composed of multiple shells of previously ejected material. If the proposed scenario is correct, then a significant fraction ($\sim 10\%$) of the most luminous SN may be self-enshrouded by dust not only before but also after the SN occurs. The spectral energy distribution of the progenitor of such an SN would be a slightly cooler version of η Carinae peaking at $20\text{--}30 \mu\text{m}$.

Key words: galaxies: irregular – infrared: galaxies – supernovae: general – supernovae: individual (SDWFS-MT-1, SN 2007va)

Online-only material: color figure

1. INTRODUCTION

The first truly large variability survey of extragalactic sources at mid-infrared (mid-IR, $3.6\text{--}8.0 \mu\text{m}$) wavelengths is the *Spitzer* Deep, Wide-Field Survey (SDWFS; Ashby et al. 2009) of the NOAO Deep Wide-Field Survey (NDWFS; Jannuzi & Dey 1999) Boötes field. The survey spans the years 2004–2008 with four epochs, covers 8 deg^2 , and contains variability statistics for nearly half a million sources (Kozłowski et al. 2010a). While the majority ($\sim 76\%$) of the extragalactic variable objects in the mid-IR are active galactic nuclei (AGNs), there is room for serendipitous discoveries such as supernovae (SNe).

In general, SDWFS was not expected to be interesting for SNe searches. First, the contrast between SNe and their hosts is relatively poor in the mid-IR, essentially because of differences in the effective temperatures. If we match the bolometric luminosities of an SN and a typical host galaxy spectral energy distribution (SED), the SN contributes $\sim 70\%$ of the V -band flux but only $\sim 8\%$ of the $3.6 \mu\text{m}$ flux. Second, with only four epochs of data, we expected SDWFS would add little to our

understanding of SNe even if one were detected. Third, the expected rates are very low. Typical Type Ia (Iip) SNe peak at $M_{[3.6]} \sim M_K \sim -18.4$ (-18.1) mag (e.g., Krisciunas et al. 2004; Maguire et al. 2010), so SDWFS can detect them in a single epoch only for redshifts $z \lesssim 0.07$ (0.06). Given the SNe Ia rates from the SDSS-II Supernova Survey (Dilday et al. 2010) and SNe Type II rate (Horiuchi et al. 2009), we would then expect to detect only of order 1 Type Ia SN and of order 7 Type II SNe in the SDWFS survey even if we could safely search for them at the 5σ detection level for a single epoch ($[3.6] = 19.1$ mag). In practice, controlling the false positive rates for identifying variable sources means that the variability selection criteria must be significantly more conservative than a 5σ peak at the detection limit (see Kozłowski et al. 2010a), so we did not expect to detect any SNe in SDWFS.

There is a subclass of Type IIIn SNe that are far more luminous, reaching $M_{[3.6]} \sim M_K \sim -20$ mag (e.g., Mannucci et al. 2003), which we could detect up to $z \simeq 0.15$. The leading theory for these SNe uses collisions between two massive shells of material to efficiently radiate the kinetic energy of the SN in the optical (Smith & McCray 2007; Woosley et al. 2007). The fast

¹⁴ Hubble, Carnegie–Princeton Fellow.

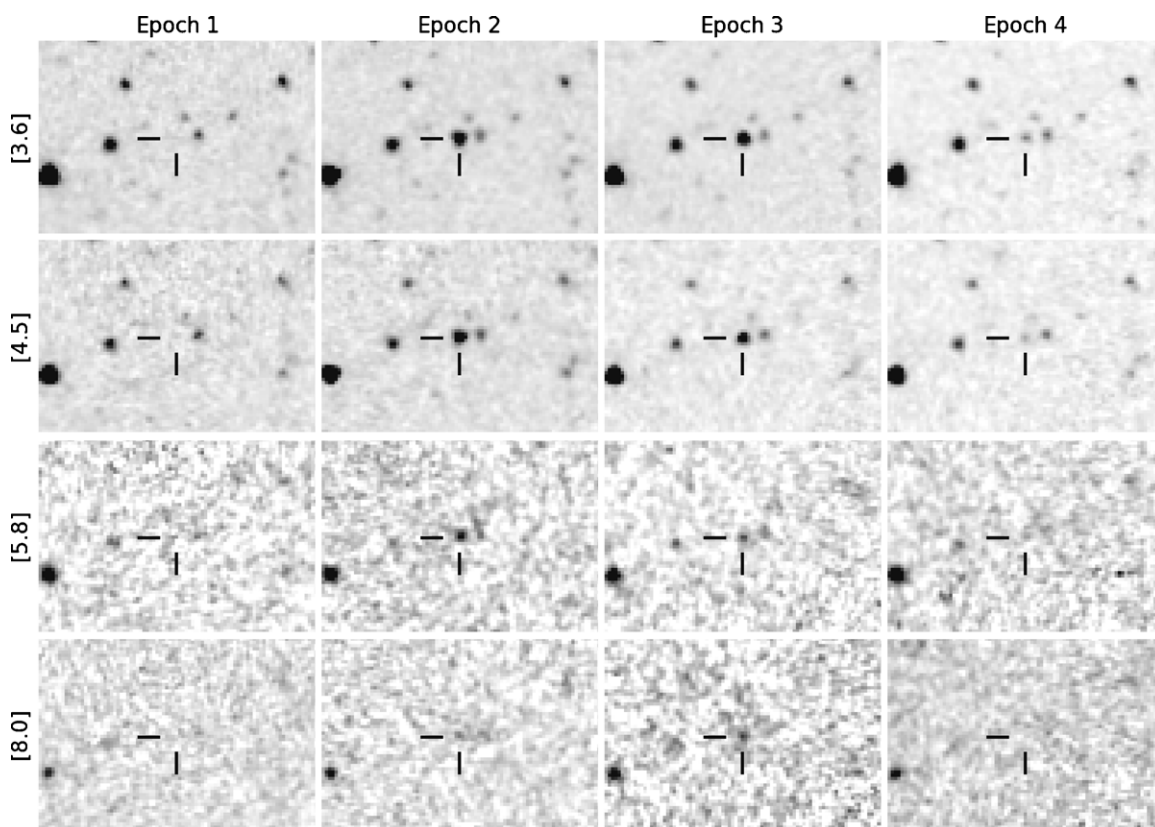


Figure 1. SDWFS images, approximately 1.5×1 arcmin², centered on the transient. The rows correspond to the [3.6], [4.5], [5.8], and [8.0] bands (downward from top), and the columns show epochs 1 through 4 (left to right), taken in 2004, 2007, and twice in 2008, respectively. The object is marked with the cross hairs. The source is clearly absent in epoch 1 and then present in all subsequent epochs except for the epoch 4 [8.0] data.

moving SN ejecta collides with an outer, slower moving shell on scales of order 10^2 AU where the optical depth is high enough to produce a well-defined photosphere but low enough for the thermal energy from the shock to be radiated before adiabatic expansion converts it back into kinetic energy. But these SNe are rare, representing only $\lesssim 1/160$ of the local Type II SNe rate (Miller et al. 2009), which more than balances the increased detection volume.

Here we investigate the nature of the brightest mid-IR transient in SDWFS. Over a 6 month period, this $z \simeq 0.2$ source radiated $\sim 10^{51}$ erg at a blackbody temperature of ~ 1350 K. In Section 2, we present the available UV, optical, and mid-IR data along with a Keck spectrum of the host galaxy. Then, in Section 3, we consider a range of possible scenarios for producing this source and conclude that a simple variant of the models for the hyper-luminous Type II In SNe is the best explanation for this source. The paper is summarized in Section 4. Throughout this paper, we use a standard Λ -cold dark matter (Λ CDM) model with $(\Omega_\Lambda, \Omega_M, \Omega_k) = (0.73, 0.27, 0.0)$ and $h = H_0/100 = 0.71$.¹⁵ All magnitudes are in the Vega system.

2. DATA

2.1. Spitzer/IRAC Data

SDWFS-MT-1 (aka SN 2007va; Kozłowski et al. 2010b), where MT means mid-IR transient as a parallel notation to using

OT for optical transient, is the most significantly variable source in the entire SDWFS field. It corresponds to the SDWFS source SDWFS J142623.24 + 353529.1. The [3.6] and [4.5] light curves were strongly correlated ($r = 1$) and the variability amplitude was 76 standard deviations from the mean for its average magnitude. A detailed definition of these variability criteria is given in Kozłowski et al. (2010a). The SDWFS survey consists of four epochs, taken 3.5 years, 6 months, and 1 month apart. The object is not detected in any of the four IRAC bands in the first epoch (also known as the IRAC Shallow Survey; Eisenhardt et al. 2004) on 2004 January 10–14 (JD' = JD - 24, 500, 00 \approx 3016.5). The SDWFS single epoch 3σ detection limits of [3.6] = 19.67 mag, [4.5] = 18.73 mag, [5.8] = 16.33 mag, and [8.0] = 15.67 mag ($4''$ apertures corrected to $24''$; Vega mag), set our upper limits on the object brightness in the first epoch. The observed part of the transient peaked in the second epoch taken 2007 August 8–13 (JD' \approx 4322.5) at [3.6] = 15.93 mag and [4.5] = 15.61 mag (Figures 1 and 2). It was slightly fainter 6 months later in epoch 3 (2008 February 2–6, JD' \approx 4500.5), with [3.6] = 16.09 mag and [4.5] = 15.76 mag. Then, in a matter of a month, the object faded by almost 2 mag to [3.6] = 17.99 mag and [4.5] = 17.72 mag in epoch 4 on 2008 March 6–10 (JD' \approx 4533.5). We present all the available *Spitzer* data in Table 1.

IRAC (Fazio et al. 2004) simultaneously observes the [3.6]/[5.8] or [4.5]/[8.0] bands, and in SDWFS the [4.5]/[8.0] observations were taken 40 s after the [3.6]/[5.8] ones. Each epoch consists of three 30 s exposures in each band, taken no more than 2 days apart, and the images for the whole mosaics were taken within 5 days. We confirmed that the transient was

¹⁵ To derive basic parameters of the transient and its host galaxy, we used the cosmology calculator (Wright 2006); <http://www.astro.ucla.edu/~wright/CosmoCalc.html>.

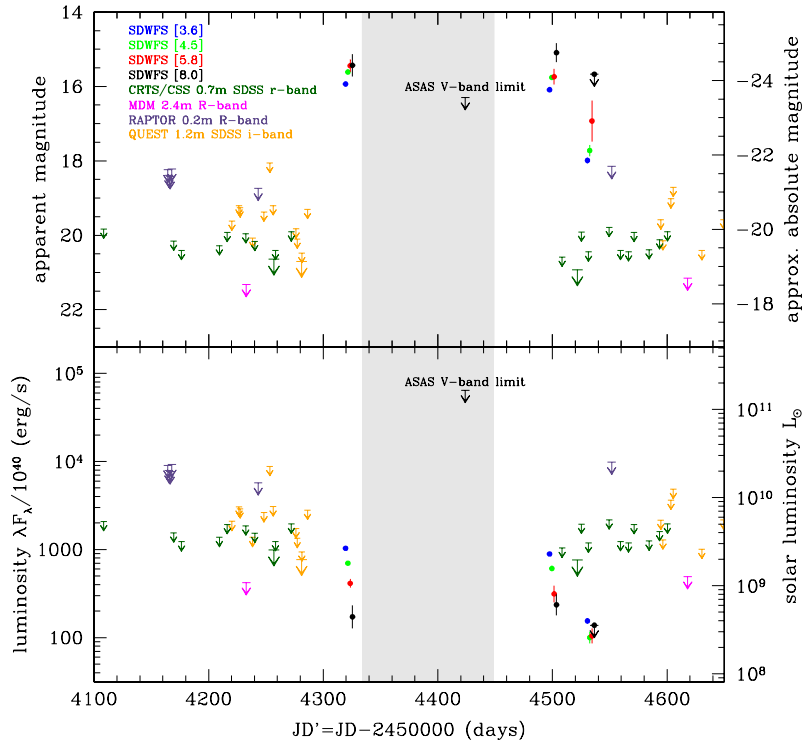


Figure 2. Light curves of the transient. Top panel: observed optical and mid-IR magnitudes. For display purposes, the IRAC points are offset by -3 days [3.6], -1 day [4.5], $+1$ day [5.8], and $+3$ days [8.0]. The right y-axis shows the absolute magnitudes without K -corrections. A normal Type II SN would peak at $M \simeq -20$ mag at $3.6 \mu\text{m}$. The gray area marks the region when the mid-IR transient was not visible to airmass < 1.5 . The large dark green symbols mark the CRTS upper limits found by stacking the three nearest epochs (small symbols) into one image. The RAPTOR upper limits (purple symbols) are stacks of 21–62 images. The QUEST upper limits (orange) are derived based on 1–4 stacked images per epoch. The large symbol for QUEST combines the four nearest epochs. Bottom panel: points from the upper panel converted to luminosity as λF_λ .

(A color version of this figure is available in the online journal.)

Table 1
SDWFS Mid-IR Data in the Observed Frame

| Band (Units) | Epoch 1 | Epoch 2 | Epoch 3 | Epoch 4 |
|--|----------|------------------|------------------|------------------|
| [3.6] (mag) | >19.67 | 15.93 ± 0.01 | 16.09 ± 0.01 | 17.99 ± 0.08 |
| [4.5] (mag) | >18.73 | 15.61 ± 0.02 | 15.76 ± 0.03 | 17.72 ± 0.15 |
| [5.8] (mag) | >16.33 | 15.44 ± 0.15 | 15.74 ± 0.21 | 16.93 ± 0.55 |
| [8.0] (mag) | >15.67 | 15.43 ± 0.30 | 15.09 ± 0.26 | >15.67 |
| λF_λ ([3.6]) ($10^{40} \text{ erg s}^{-1}$) | <32 | 1017 ± 18 | 878 ± 15 | 153 ± 11 |
| λF_λ ([4.5]) ($10^{40} \text{ erg s}^{-1}$) | <39 | 690 ± 16 | 601 ± 19 | 99 ± 14 |
| λF_λ ([5.8]) ($10^{40} \text{ erg s}^{-1}$) | <179 | 406 ± 42 | 308 ± 61 | 103 ± 55 |
| λF_λ ([8.0]) ($10^{40} \text{ erg s}^{-1}$) | <133 | 166 ± 47 | 227 ± 55 | <133 |
| Blackbody fit including dust emissivity ($Q \propto \lambda^{-1}$) | | | | |
| $E_{\text{rad}} > 0.9 \times 10^{51} \text{ erg}$ | | | | |
| Blackbody Temp. (K) | ... | 1357 ± 57 | 1338 ± 71 | 1400 ± 353 |
| “Total” L ($10^{43} \text{ erg s}^{-1}$) | ... | ~ 6.8 | ~ 5.7 | ~ 1.8 |
| Radius R (AU) ^a | ... | ~ 11000 | ~ 10500 | ~ 5500 |

Notes. The SDWFS magnitudes were measured in $4''$ diameter aperture with aperture corrections to $24''$.

^a Radius R corresponds to the radius where the optical depth $\tau_{\text{optical}} \approx 1$.

present in the individual artifact-corrected basic calibrated data (CBCD) frames corresponding to the position of the transient. The mosaic image for each epoch is then a combination of three to four of these frames, and there is no indication of problems in the SDWFS reductions (see Ashby et al. 2009).

2.2. Keck Spectrum

We obtained a Keck/LRIS (Oke et al. 1995) spectrum of the transient’s host galaxy on 2010 March 12, long after the transient was gone. The spectrum (shown in Figure 3) shows clear

emission lines of $\text{H}\alpha$, $\text{H}\beta$, $\text{H}\gamma$, $\text{H}\delta$, $\text{H}\epsilon$, and $\text{H}\zeta$, $[\text{O II}]$ at 3727 \AA , $[\text{O III}]$ at 4363 \AA , 4959 \AA , and 5007 \AA , and $[\text{Ne III}]$ at 3869 \AA and 3968 \AA . The redshift of the host galaxy is $z = 0.1907$, so the luminosity distance is 920 Mpc, the distance modulus is 39.82 mag, and the angular scale is $3.15 \text{ kpc arcsec}^{-1}$. Before measuring the line fluxes, we corrected the host galaxy spectrum for Galactic extinction ($E(B - V) = 0.014 \text{ mag}$) using Schlegel et al. (1998). We do not detect the $[\text{N II}]$ 6584 \AA line, which implies $\log([\text{N II}]/\text{H}\alpha) < -1.5$. Combining it with $\log([\text{O III}] 5007 \text{ \AA}/\text{H}\beta) = 0.78$, we conclude that the host is an irregular

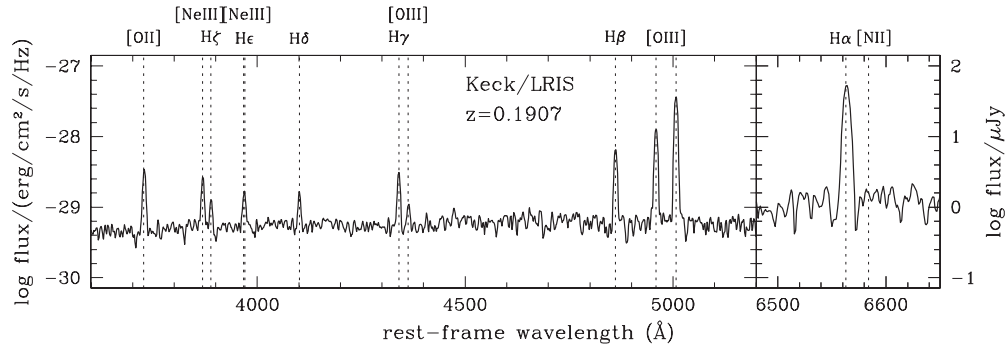


Figure 3. Keck/LRIS rest-frame spectrum (selected parts) of the transient’s host galaxy with the major emission lines marked. From the line positions, we find a redshift of $z = 0.1907$. To derive the metallicity, we measured the fluxes of the [O II] 3727 Å, [O III] 4363 Å, [O III] 4959 Å, [O III] 5007 Å, and H β 4861 Å lines.

H II galaxy (see, e.g., Terlevich et al. 1991; Kniazev et al. 2004). The lack of [N II] and [Ne v] 3426 Å lines and the clear detection of the 4363 Å line rule out the presence of an AGN.

We followed the prescription of Pilyugin & Thuan (2007) to derive the gas-phase oxygen abundance of the host. We measured the fluxes of the [O II] 3727 Å, [O III] 4363 Å, [O III] 4959 Å, [O III] 5007 Å, and H β 4861 Å emission lines to find a metallicity of $12 + \log(\text{O}/\text{H}) = 7.85 \pm 0.13$. We assumed an electron density of $n_e = 100 \text{ cm}^{-3}$, but the value does not change significantly with changes in the electron density (e.g., $12 + \log(\text{O}/\text{H}) = 7.87$ if we use $n_e = 1000 \text{ cm}^{-3}$ instead). Next, we verified this metallicity measurement using the prescriptions of Izotov et al. (2006) to get $12 + \log(\text{O}/\text{H}) = 7.79$. As a cross-check, we also used the oxygen-to-hydrogen flux ratio $R_{23} = ([\text{O II}] + [\text{O III}])/\text{H}\beta = (F_{\lambda 3727} + F_{\lambda 4959} + F_{\lambda 5007})/F_{\lambda 4861}$ method of Pagel et al. (1979) and the Pettini & Pagel (2004) O3N2 method to derive oxygen abundances. The clear detection of the 4363 Å line and $\log([\text{N II}]/\text{H}\alpha) < -1.5$ strongly suggests that we should use the “lower” metallicity branch in the R_{23} method. We use the relations from Skillman (1989) and Yin et al. (2007) with our measured $\log(R_{23}) = 0.94$ to get oxygen abundances of $12 + \log(\text{O}/\text{H}) = 7.78$ and 7.80, respectively. The O3N2 method gives $12 + \log(\text{O}/\text{H}) < 8.0$. All these estimates are approximately 10% of the solar value (assuming 8.8 from Delahaye et al. (2010)).

2.3. UV and Optical Data

In order to understand the origin of this mid-IR transient, we searched for any available UV and optical data for this area of the sky in the relevant time span.

The host galaxy was detected in the original NDWFS (Jannuzi & Dey 1999) with $B_W = 23.98 \pm 0.05 \text{ mag}$ ($\lambda F_\lambda = 6.64 \times 10^{41} \text{ erg s}^{-1}$), $R = 22.78 \pm 0.05 \text{ mag}$ ($1.10 \times 10^{42} \text{ erg s}^{-1}$), and $I = 22.58 \pm 0.09 \text{ mag}$ ($8.39 \times 10^{41} \text{ erg s}^{-1}$). It was unresolved in $1''.2$ (FWHM) seeing, which puts an upper limit on the size of the galaxy of 3.8 kpc. In archival *Galaxy Evolution Explorer* (GALEX; Morrissey et al. 2007) data, the host has $\text{NUV} = 24.30 \pm 0.17 \text{ mag}$ and no detection in FUV. The GALEX source is formally $0''.87$ from the SDWFS/NDWFS source, but there are no other blue sources within $20''$. Both the colors of the host and its size are consistent with a blue, low-luminosity, low-metallicity galaxy. We used the template model of an irregular galaxy from Assef et al. (2010) to estimate the mid-IR magnitudes of the host. Fitting the GALEX NUV, and NDWFS B_W , R , and I -band magnitudes of the host galaxy, and assuming $z = 0.1907$, the expected apparent (absolute) IRAC magnitudes are $[3.6] = 20.87(-18.56) \text{ mag}$, $[4.5] = 20.69(-18.57) \text{ mag}$,

$[5.8] = 20.52(-20.02) \text{ mag}$, and $[8.0] = 18.37(-21.45) \text{ mag}$. This is consistent with the failure to detect the host in the first SDWFS epoch. We estimate rest-frame host luminosities of $M_B = -16.11 \text{ mag}$ and $M_R = -16.75 \text{ mag}$, making this an $L/L_\star \simeq 0.01$ galaxy (Karachentsev 2005).

Although the field was monitored by at least five optical variability surveys, the peak of the transient occurred when the field was “behind” the Sun, so almost all the optical data correspond to the periods before epoch 2 and after epoch 4. The Boötes field was observed seven times between $\text{JD}' = 3800$ and 4620 with the $8\text{k} \times 8\text{k}$ Mosaic CCD camera on the 2.4 m MDM Hiltner Telescope. The two most interesting observations took place 90 days before the second and 84 days after the fourth SDWFS epoch, bracketing the period of the transient. In these 180 s exposures, we detected no flux from the transient (or the host) at a 3σ level of $R = 21.32 \text{ mag}$ ($4.2 \times 10^{42} \text{ erg s}^{-1}$) and 21.15 mag ($4.9 \times 10^{42} \text{ erg s}^{-1}$), respectively.

The Catalina Sky Survey (CSS; Larson et al. 2003)/Catalina Real-Time Transient Survey (CRTS; Drake et al. 2009) provides light curves for the period prior to epoch 2 and overlapping epochs 3 and 4. Each epoch of four 30 s exposures on the 0.7 m Catalina Schmidt Telescope reaches an r -band magnitude limit of $\sim 20 \text{ mag}$. These data provide the strongest limit on the optical-to-mid-IR flux ratios, where a stack of 12 images (3 epochs) gives a 3σ upper limit on the transient of $r > 20.93 \text{ mag}$, corresponding to $7.6 \times 10^{42} \text{ erg s}^{-1}$ (large dark green symbol to the right in Figure 2), in the period between epochs 3 and 4.

The QUEST (Djorgovski et al. 2008) survey further limits the optical emission before epoch 2 and after epoch 4. There are 19 epochs each consisting of 1–4, 60–100 s exposures with the 1.2 m Samuel Oschin telescope in a wide red/IR filter that we calibrated to i band. The most interesting data were taken ~ 40 days prior epoch 2, where we stacked six adjacent QUEST epochs ($\text{JD}' = 4276.71\text{--}4286.76$) to obtain 3σ detection limit of $i > 20.70 \text{ mag}$ ($7.7 \times 10^{42} \text{ erg s}^{-1}$, large orange symbol in Figure 2).

Similarly, by co-adding the high cadence RAPid Telescopes for Optical Response (RAPTOR; Woźniak et al. 2009) observations of the field, each of which is a 30 s exposure using the RAPTOR-P array of four 200 mm Canon telephoto lenses, we obtained 15 upper limits at various epochs between 2004 and 2008, before and after the transient (Figure 2). Calibrating the unfiltered observations to an R -band equivalent using Tycho 2 stars, we find no evidence for the transient, with $C_R > 18 \text{ mag}$ (3σ).

Only the northern station of the All Sky Automated Survey (ASAS) data (Pojmański 1997) obtained data during the peak

of the transient. Combining seven high-quality ASAS images during the transient ($JD' = 4322.75\text{--}4525.11$), we obtain a weak upper limit on the transient magnitude of $V > 16.3$ mag (3σ), corresponding to 6.2×10^{44} erg s^{-1} .

3. DISCUSSION OF THE TRANSIENT

The steeply falling, roughly power-law SED of the transient (Figure 4) is suggestive of thermal emission by a source cooler than normal stars. If we fit the SED as dust emission using an emissivity of $Q \propto \lambda^{-\beta}$, we find good fits with $\beta \simeq 1$ as is typical of the mid-IR emission by warm dust (e.g., Seki & Yamamoto 1980; Draine 1981; Graham & Meikle 1986). The temperature of $T \approx 1350$ K varies little between epochs (Table 1) and is below typical dust destruction temperatures of $T \gtrsim 1600$ K (e.g., Dwek 1983; Guhathakurta & Draine 1989). Table 1 summarizes these estimates of the temperatures and luminosities. A zeroth-order estimate (ignoring the dust emissivity) of the radius R of the dust photosphere is

$$R = 8000 \left(\frac{L}{10^{43} \text{ erg s}^{-1}} \right)^{1/2} \left(\frac{1000 \text{ K}}{T} \right)^2 \text{ AU}. \quad (1)$$

We are assuming that the shell is optically thick and R corresponds to the radius where the (optical) optical depth is of order unity. If the dust is optically thin, as the case for typical dust echoes, there is no characteristic radius or temperature since photons can be absorbed and emitted at any distance from the SN. We discuss these issues in more detail below. For the second and third epochs of SDWFS, with total luminosity $L \approx 6 \times 10^{43}$ erg s^{-1} and temperature $T \approx 1350$ K, we find the radius to be $R \approx 11000$ AU (0.05 pc). The total energy radiated in the IR is then $E_{\text{rad}} \approx 10^{51}$ erg. The weak optical limits mean that a comparable amount of energy might have been radiated in the optical.

We used the more sophisticated radiation transport model DUSTY (Ivezic & Elitzur 1997) to check this estimate. For incident blackbody spectra with temperatures 10,000–20,000 K, shell geometries with constant density, and dust temperatures at the inner photosphere edge of 1300–2000 K, we could match the epoch 2 and 3 SEDs, including a weak optical limit, using shells dominated by graphite, a visual optical depth of $\tau \sim 1\text{--}3$, and a radius $R \sim 10,000\text{--}40,000$ AU. Pure silicate dusts were unable to fit the data well, producing the wrong spectral shape for reasonable τ and inner dust temperatures. These results are consistent with our simple estimates and strongly suggest that there was an optical counterpart, albeit with significant extinction ($R \gtrsim 21.7$ mag).

Before outlining our preferred explanation of the transient as a self-obscured SN, we briefly outline the hypotheses we rejected.

3.1. Rejected Hypotheses

First, the transient cannot be explained by a Galactic star. The arguments against are as follows: (1) based on the Keck spectrum, we know that the source is spatially coincident with an irregular galaxy; (2) few stars can brighten by at least 5 mag (by more than 100 times) in the mid-IR and then stay at this level for 6 months before fading; and (3) most flaring stars do not flare in the mid-IR but in the UV. There are exceptions to (2) and (3), and these will generally be accreting systems where the disk can alter the spectral properties. However, the NDWFS field is a high latitude ($b \simeq 67^\circ$) field with negligible Galactic extinction

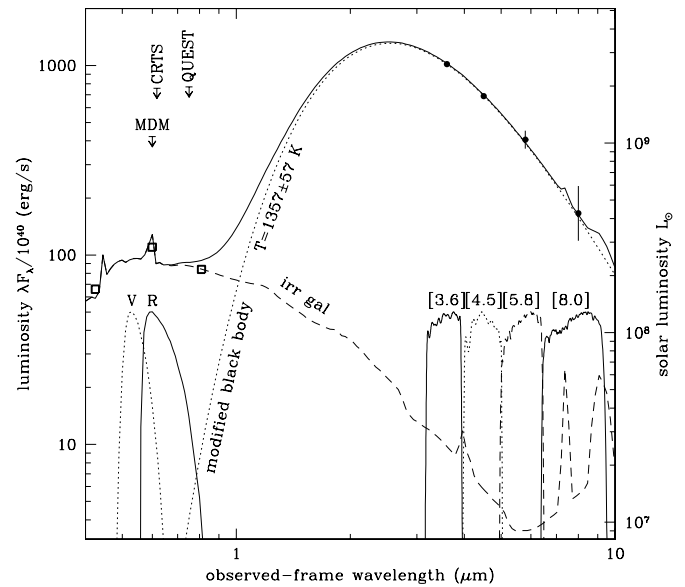


Figure 4. SED of the transient during the second epoch of SDWFS. We fit a blackbody SED that includes the dust emissivity ($Q \propto \lambda^{-1}$) to the four IRAC bands (filled circles) and find a best-fitting temperature of $T = 1357 \pm 57$ K (dotted line). We also show a template SED for the host galaxy modeled as an irregular (dashed line; Assef et al. 2010) and the combination of the modified blackbody and irregular galaxy SEDs (thick solid line). Overplotted are the V, R, and IRAC filter transmission curves, “normalized” to 5×10^{41} erg s^{-1} . The MDM (QUEST) limit is derived for an observation taken 90 (~ 40) days prior to the second epoch of SDWFS. The CRTS limit corresponds to the stack of three epochs (12×30 s images) taken between SDWFS epochs 3 and 4. The open squares mark the NDWFS B_W , R, and I-band measurements for the host galaxy (from left to right).

and unlikely to contain young (protostars) or massive (Be stars) stars with these characteristics, particularly if they must also have no optical counterpart in quiescence despite needing to be nearby sources because of the short path length out of the disk.

The second possibility is that we are really observing an AGN. First, we note that there are no signs of AGN activity in the host spectrum. The narrow lines in a galaxy are on relatively large scales and should show line ratios averaged over decades (or more) of AGN activity, so the lack of a spectrum during the transient does not invalidate using them to argue against an AGN. Moreover, the mid-IR colors at the peak of the transient, $[3.6] - [4.5] = 0.3$ mag and $[5.8] - [8.0] = 0.0$ mag (epoch 2), are inconsistent with that of an AGN (e.g., Stern et al. 2005; Assef et al. 2010; Kozłowski et al. 2010a). While the composite SED of an AGN and its host can have these colors, we know from the host flux limits in the first epoch that the SED at the peak should be dominated by the AGN, and a pure AGN at $z \simeq 0.2$ should have mid-IR colors closer to $[3.6] - [4.5] \simeq 0.8$ mag and $[5.8] - [8.0] \simeq 1.1$ mag (Assef et al. 2010). We also considered the possibility of a tidally disrupted star in the context of the super-Eddington accretion models of Loeb & Ulmer (1997). While these models have an inflated, relatively cool envelope around the black hole, the expected temperatures of $T \approx 7000 (M_{\text{BH}}/10^5 M_\odot)^{1/4}$ K for a black hole of mass M_{BH} are still too high. A black hole with low enough mass ($M_{\text{BH}} \approx 150 M_\odot$) to match the temperature ($T \approx 1350$ K) would be unable to produce the observed luminosity. The Eddington luminosity for such a low mass is only $L_{\text{Edd}} \approx 2 \times 10^{40}$ erg s^{-1} .

The third possibility is that it is a γ -ray burst (GRB). We can rule it out as direct emission from a burst because the timescale (6 months) is too long and the SED is wrong for direct

beamed emission (e.g., Sari et al. 1999). It cannot be indirect emission, where a dusty region absorbs and reradiates emission from the jet, because a relativistic jet expands past the scale of the photosphere ($\sim 10^4$ AU) too quickly (~ 60 rest-frame days) to produce the observed event duration.

Finally, this cannot be gravitational lensing of a background object by the host galaxy (see Wambsganss (2006) for a review). The timescales are such that it would have to be microlensing by the stars in the lens galaxy, but there are no known mid-IR sources that are sufficiently compact to show such a large, and apparently achromatic, degree of magnification. Moreover, almost any potential source would have to show a still stronger degree of optical magnification that would disagree even with our weak optical limits (see, e.g., Morgan et al. 2010).

3.2. An Obscured Supernova Explosion

Our working hypothesis is that SDWFS-MT-1 is an SN analogous to SN 2006gy, an extremely luminous Type II_n SN (Ofek et al. 2007; Smith et al. 2007, 2008b, 2010; Smith & McCray 2007; Miller et al. 2010). SN 2006gy peaked at $M_V \simeq -22$ mag, corresponding to a luminosity of $L \sim 3 \times 10^{44}$ erg s^{-1} , and it radiated of order $E_{\text{rad}} > 2 \times 10^{51}$ erg in total (Ofek et al. 2007; Miller et al. 2010). In a normal Type II SN, a very small fraction ($\lesssim 1\%$) of the available energy is radiated. The initial energy from the shock is converted into kinetic energy by adiabatic expansion, leaving little to power the luminosity. Thus, an SN ejecting $M_{\text{ej}} \sim 10 M_{\odot}$ at velocities of $v_{\text{ej}} \sim 4000$ km s^{-1} contains enough kinetic energy, $E_{\text{kin}} \simeq 2 \times 10^{51}$ erg to power the transient, but it is only radiated on timescales of order 10^3 years as the SN remnant develops. The scenario we present was proposed by Smith & McCray (2007) for SN 2006gy with further elaborations in Smith et al. (2008b) and Miller et al. (2010).

Very massive stars ($\gtrsim 50 M_{\odot}$) are known to undergo impulsive events ejecting significant fractions of the stellar envelope. The most famous example is the eruption of η Carinae in 1837–1857 (see Davidson & Humphreys 1997), but it also includes some of the so-called “supernova impostors” (e.g., Smith & Owocki 2006; Pastorello et al. 2007). The number and temporal distributions of these mass ejections relative to the final SN are unknown, but there are several cases where one seems to have occurred shortly before the final SN (e.g., Smith et al. 2007). Pair instability SNe can also produce a sequence of mass ejections just prior to the death of the star (see Woosley et al. 2007). Let us suppose that the progenitor of SDWFS-MT-1 was such a massive star and had two such eruptions in its final phases, roughly 300 and 5 years before the final explosion, each of which ejected of order $M_{\text{shell}} \simeq 10 M_{\odot}$. For a typical ejection velocity of 200 km s^{-1} (e.g., Smith & Owocki 2006), these shells would lie roughly 13000 and 200 AU from the star when it exploded.

The role of the first shell is to convert the kinetic energy of the explosion into radiation following Smith & McCray (2007). Roughly speaking, the collision between the ejected material and the first shell can extract fraction $M_{\text{shell}}/(M_{\text{ej}} + M_{\text{shell}})$ of the kinetic energy and convert it to radiation. The distance to the shell is tuned so that the shock crossing time is comparable to the Thomson photon diffusion time, thereby allowing the radiation to escape without significant adiabatic losses. This requires a total mass of approximately $M = 4\pi R^2 m_p c / \sigma_T v_{\text{ej}} = 2.6 R_{100}^2 v_{\text{ej},4000}^{-1} M_{\odot}$, where $R = 100 R_{100}$ AU and $v_{\text{ej}} = 4000 v_{\text{ej},4000}$ km s^{-1} . We can get up to $20 M_{\odot}$ either by making

$R \simeq 300$ AU or by allowing for adiabatic losses. This then implies characteristic time, energy, luminosity, and temperature scales of $t = R/v_{\text{ej}} = 50 R_{100}/v_{\text{ej},4000}$ days, $E = (1/4) M v_{\text{ej}}^2 = 2 \times 10^{50} R_{100}^2 v_{\text{ej},4000}$ erg, $E/t = 5 \times 10^{43} v_{\text{ej},4000}^2 R_{100}$ erg s^{-1} , and $T = (L/4\pi R^2 \sigma)^{1/4} = 14,000 v_{\text{ej},4000}^{1/2} R_{100}^{-1/4}$ K, respectively, where we have used the estimate of the total mass and equally divided it between the shell and the SN ejecta. The basic energetics, but not the radiation transport, are largely confirmed by the simulations of van Marle et al. (2009). This set our choice of incident temperature in the DUSTY models. Thus, a shell of ejected material at $R \sim 300 v_{\text{ej},4000}^{-1}$ AU can produce the necessary energetics and luminosities but cannot match the observed timescales (too short) or temperatures (too high).

The role of the second shell is to match the time and temperature scales. Smith et al. (2008b) and Miller et al. (2010) invoke a second $M_{\text{shell}} \simeq 10 M_{\odot}$ shell located at $R \simeq 1$ pc in order to explain the relatively bright, long-lived IR emission observed for SN 2006gy. Their shell is, however, optically thin to optical light ($\tau \simeq 0.02$) because the total infrared emission is only a small fraction of the total. The optical depth of a shell is of order $\tau \simeq 0.1 \kappa (M_{\text{shell}}/10 M_{\odot}) (10^4 \text{ AU}/R)^2$ for κ in $\text{cm}^2 \text{ g}^{-1}$, which leads to an optically thin shell with $\tau_{\text{opt}} \simeq 0.08$ for an $R \simeq 1$ pc shell radius and $\kappa_{\text{opt}} \simeq 500 \text{ cm}^2 \text{ g}^{-1}$ for a radiation temperature of order 10^4 K (e.g., Semenov et al. 2003). This opacity, $\kappa \simeq 500 \text{ cm}^2 \text{ g}^{-1}$, corresponds to a dust-to-gas ratio of approximately 1%, which arguably may be high for a low-metallicity galaxy. Note, however, that SN 2006gy is probably also associated with a low-metallicity galaxy (see Section 3.4) and the shell producing its dust echo contains enough dust for our scenario.

To explain SDWFS-MT-1, we simply move the shell inward. At this point, however, we should improve on Equation (1) with a simple model for an optically thick dust echo. Suppose that the dust lies in an optically thick spherical shell of radius R and is exposed to luminosity L_p for a period of time t_p . Because all the dust is exposed to the same luminosity, the dust temperature is independent of position or time while irradiated. The observer, however, sees the luminosity pulse modulated by the light travel time $2R/c$ across the shell. In this simple model, the light curves are trapezoids with linear rises and falls, connected by a plateau, created by the changing fraction of the shell, illuminated by the outburst from the observer’s perspective, but the dust temperature is constant. Models that can reproduce the drop in luminosity between epochs 3 and 4 have the pulse time $t_p < 2R/c$, with the simplest model having the luminosity plateau run from epoch 2 to epoch 3. The plateau duration is $2R/c - t_p = 180$ days, while the rises and falls last t_p . The luminosity of the plateau is $2\pi R c t_p \sigma T^4$, which is smaller than $L_p = 4\pi R^2 \sigma T^4$ by the ratio $2t_p/Rc \simeq 0.2$ between the light crossing time and the pulse length (if $t_p > 2R/c$, the plateau luminosity is L_p). The factor of 3 drop in luminosity between epochs 3 and 4 is $L_4/L_3 = 1 - t_{34}/t_p \simeq 1/3$, where $t_{34} \simeq 33$ days is the time between these epochs. Thus, we have $t_p \simeq 50$ days and $R \simeq 19000$ AU or 115 light days. With these time and distance scales, we come close to matching the epoch 2 and 3 luminosities given the observed temperatures, with an estimated luminosity of $L_2 = L_3 = 5 \times 10^{43}$ erg s^{-1} . The true luminosity is $L_p \simeq 2 \times 10^{44}$ erg s^{-1} , which is why the radius estimate is somewhat larger than the estimates of Equation (1). There is some tension between the plateau luminosity and the drop in luminosity between the last two epochs, but the overall

agreement is good given the crudeness of the model both for the dust emission and the luminosity profiles.

The mass required to produce a shell with optical depth τ at this distance is $M \simeq \tau(\kappa/500 \text{ cm}^2 \text{ g}^{-1})(R/19,000 \text{ AU})^2 M_\odot$, so there is little difficulty having an optically thick shell for masses of order 1–10 M_\odot even if the dust-to-gas ratio needs to be significantly reduced from $\sim 1\%$ because of the low metallicity of the galaxy. While the dust temperature is close to that for destroying dust (e.g., Dwek & Werner 1981), the situation is somewhat different from a normal SN because the (Thomson) optically thick inner shell protects the outer from any initial high-luminosity bursts of hard radiation. For the IR radiation, $\kappa_{\text{IR}} \simeq 10 \text{ cm}^2 \text{ g}^{-1}$, and the shell is optically thin to the mid-IR emission for reasonable shell masses, so the dust emission streams freely to the observer. Given the estimated pulse duration, $t_p \simeq 50$ days, and luminosity, $L_p = 2 \times 10^{44} \text{ erg s}^{-1}$, we can estimate that the inner shell is at $R \simeq 160 \text{ AU}$, the velocity must be $v_{\text{ej}} \simeq 6300 \text{ km s}^{-1}$, and the mass involved must be $M \simeq 4 M_\odot$, where the rapid decline pushes these values to small radii/masses and high velocities in order to keep t_p short. Given the crudeness of the model, it is remarkable how well all the observational features can be matched using relatively sensible physical parameters.

3.3. The Transient's Host Galaxy

The nature of the host galaxy indirectly supports this hypothesis because both GRBs and most hyper-luminous Type II SNe are also associated with low-luminosity, low-metallicity dwarf galaxies. Figure 5, similar to Figure 1 in Stanek et al. (2006), shows the position of the host galaxy for SDWFS-MT-1 in the metallicity–luminosity plane in relation to $\sim 126,000$ star-forming SDSS DR4 galaxies (Tremonti et al. 2004; Adelmann-McCarthy et al. 2006; Prieto et al. 2008). We also include the hosts of six local ($z < 0.25$) GRBs using updated estimates from Levesque et al. (2010) and including the host of GRB 100316D (Chornock et al. 2010; Starling et al. 2010). While SDWFS-MT-1 was not a GRB, its occurrence in a very low metallicity galaxy is striking, since such galaxies produce only a small fraction of massive stars in the local universe (e.g., see Figure 2 in Stanek et al. 2006). In Figure 5, we ignore small ($\lesssim 20\%$) effects on metallicity measurements arising from the method being used to derive it (see Kewley & Ellison 2008).

In fact, the hosts of most other hyper-luminous SNe also tend to be of very low luminosity ($\sim 0.01 L_*$), suggestive of their low metallicity (unfortunately, oxygen abundances have not been measured for most of these hosts). SN 2005ap (Quimby et al. 2007) at $z = 0.283$ peaked at unfiltered magnitude of $M = -22.7$ mag and is associated with an $M_R = -16.8$ ($M_B \approx -16.1$) mag dwarf galaxy. SN 2006tf (Quimby et al. 2007; Smith et al. 2008a) at $z = 0.074$ exploded in a host of low-luminosity $M_r = -16.9$ ($M_B \approx -16.2$) mag. The over-luminous $M_R = -21.3$ mag Type Ic SN 2007bi exploded in a faint, $M_B = -16.3$ mag dwarf galaxy, with $12 + \log(\text{O}/\text{H}) = 8.18 \pm 0.17$ (Gal-Yam et al. 2009; Young et al. 2010). SN 2008es at $z = 0.213$ (Miller et al. 2009; Gezari et al. 2009) reached $M_V = -22.3$ mag and exploded in a host which was not detected down to a faint luminosity of $M_V > -17.4$ ($M_B > -17.1$) mag. SN 2008fz at $z = 0.133$ peaked at $M_V = -22.3$ mag, but no host has been detected down to an upper limit of $M_R > -17$ ($M_B > -16.6$) mag (Drake et al. 2010). SN 2006gy (Quimby 2006; Smith et al. 2007; Ofek et al. 2007) is one of the two exceptions here, as it exploded in a fairly luminous S0 galaxy, NGC 1260 with $M_B \approx -20.3$ mag.

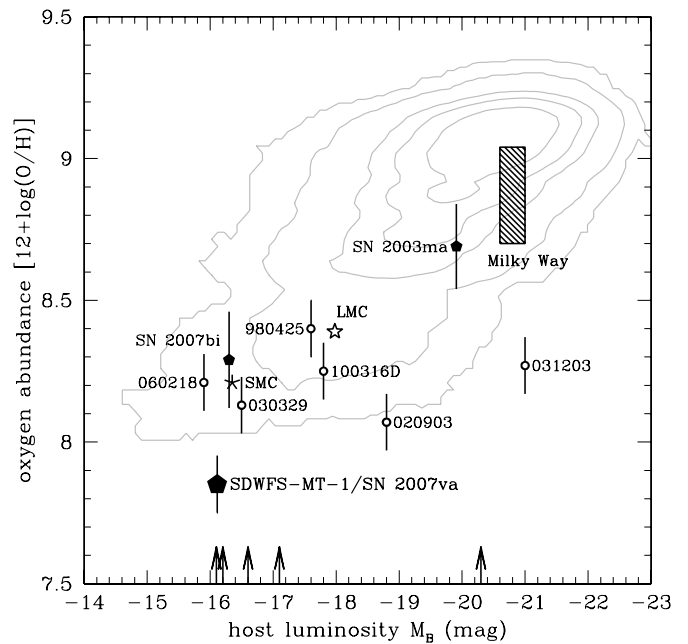


Figure 5. Metallicity–luminosity relation for 125,958 SDSS DR4 star-forming galaxies (e.g., Tremonti et al. 2004; Prieto et al. 2008). They are binned into 0.1 mag and 0.025 dex bins and the smoothed contours (3×3 bins) are drawn for 1, 10, 50, 100, and 200 objects per bin, counting from the outer contour. The figure is analogous to Figure 1 from Stanek et al. (2006). SDWFS-MT-1 is shown as the filled pentagon (lower left). A handful of local GRBs with associated SNe (and two SNe) with known host metallicities and luminosities are shown with open circles (small pentagons). The arrows show M_B for five host galaxies of high-luminosity SNe with unknown oxygen abundances. They are, from left to right, SN 2005ap, SN 2006tf, SN 2008fz, SN 2008es, and SN 2006gy (see Section 3.3). The Large Magellanic Cloud/Small Magellanic Cloud oxygen abundances are adopted following Peeples et al. (2008) and the Milky Way’s (solar) are from Delahaye et al. (2010), while the absolute magnitudes are from Karachentsev (2005).

Another example is SN 2003ma (Rest et al. 2009) that released $4 \times 10^{51} \text{ erg}$ in an $M_B \approx -19.9$ mag, $12 + \log(\text{O}/\text{H}) \approx 8.7$ galaxy.

The general message is clear: GRBs and luminous SNe prefer low-metallicity, low-luminosity galaxies, so does SDWFS-MT-1.

3.4. Rates

We systematically searched for transients similar to SDWFS-MT-1 and SNe in general in the SDWFS data. We considered highly correlated [3.6] and [4.5] light curves ($r > 0.8$) with flag = 1 (photometry unaffected by the wings of bright stars), variability significances $\sigma_{[3.6]} > 1$ and $\sigma_{[4.5]} > 1$ and colors $[3.6] - [4.5] < 0.4$ to eliminate AGNs (see Kozłowski et al. 2010a). We selected as candidate objects that at their peak were brighter than $[3.6] < 18.67$ mag, corresponding to 1 mag brighter than the 3σ detection limit, and which changed in brightness by at least 1 mag between either epochs 1 and 2 or epochs 2 and 3/4. The latter two epochs are close enough together that an SN might not show a significant brightness change between them. We found six candidate objects, one of which is SDWFS-MT-1. Four are artifacts due to PSF structures (long spikes) from bright stars.

The remaining object, SDWFS J142557.64+330732.6 (hereafter SDWFS-MT-2), peaks in epoch 2 close to our selection limit at $[3.6] = 18.52 \pm 0.14$ mag and $[4.5] = 18.71 \pm 0.33$ mag. It lies $0^\circ 7'$ south–west of a potential host galaxy with *GALEX* $\text{NUV} = 24.02 \pm 0.19$ mag, *NDWFS* $B_W = 23.77 \pm 0.03$ mag,

$R = 23.34 \pm 0.04$ mag, and $I = 22.68 \pm 0.06$ mag that is not detected in SDWFS. In the deep images from NDWFS, the host galaxy appears to be an extended, possibly edge-on (length $3''.0$ in $1''/2$ seeing) disk, with a redder core and bluer outer regions. The transient lies in the bluer outer regions, although its position is only known to $\sim 0''.2$ due to its faintness. We estimate a photometric redshift of $z \approx 1.0$ for the host using the template models of Assef et al. (2010), corresponding to a comoving distance of 6.6 Gpc and a linear scale of $8.0 \text{ kpc arcsec}^{-1}$. This translates into the linear diameter of the host of ~ 24 kpc. The best-fit model for the SED of the host is a mixture of an AGN and a starburst template. The mid-IR color of the transient, $[3.6] - [4.5] = 0.2 \pm 0.5$ mag, is ambiguous on the question of an SN or AGN origin for the transient, although the offset position would favor an SN. Given the redshift estimate, however, the implied luminosity is too high even for the brightest normal SN—for $M_{[3.6]} \sim M_K \sim -20$ mag (Mannucci et al. 2003), the peak magnitude of $[3.6] \sim 24$ mag would be far below our detection limits. A second event like SWFS-MT-1 would have to be even more extreme. Given the paucity of the data, interpreting this source as a false positive seems the most probable explanation.

For events with 6 month durations like SDWFS-MT-1, our survey time coverage is approximately $\Delta T = 2$ years. SDWFS-MT-1 peaked in epoch 2 at fluxes of 0.12 mJy in $[3.6]$ and 0.10 mJy in $[4.5]$ at a luminosity distance of 920 Mpc. The peak flux limit for our systematic search is $9.6 \mu\text{Jy}$ (5σ in $[4.5]$) which means we could have detected SDWFS-MT-1 at a luminosity distance of 3000 Mpc ($920 \times (100/9.6)^{1/2}$) or about $z = 0.52$ ignoring K -corrections, which will initially aid detection because the SED peaks blueward of the IRAC bands. Thus, we could detect the source in a comoving volume of approximately $V = 6 \times 10^6 \text{ Mpc}^3$. Combining these factors, we estimate a rate for SDWFS-MT-1-like transients of $r = (V\Delta T)^{-1} \sim 8 \times 10^{-8} \text{ Mpc}^{-3} \text{ yr}^{-1}$ where we have not corrected the timescales for redshifting effects given the otherwise large uncertainties from the statistics of one event. This is approximately 10^{-3} of the Type II SNe rate (Horiuchi et al. 2009), ~ 0.1 of the hyper-luminous Type II SNe (Miller et al. 2009), and ~ 10 of the GRB rate (Nakar 2007).

4. SUMMARY

In this paper, we presented the discovery of a luminous mid-IR transient, SDWFS-MT-1, that is unusual in several ways. Its most striking features are the high luminosity, $L \sim 6 \times 10^{43} \text{ erg s}^{-1}$, the low apparent temperature, $T \sim 1350 \text{ K}$, the long, 6 month duration of the event, and the resulting high amount of radiated energy, $E_{\text{rad}} \gtrsim 10^{51} \text{ erg}$. A model that explains the transient is a self-observed SN, that has two concentric (patchy) shells, each with the mass of $\sim 10 M_{\odot}$, ejected prior to the SN explosion. The inner shell at $\sim 150 \text{ AU}$ protects the dust in the outer shell from initial luminosity spikes and converts the high kinetic energy of the SN shock wave into thermalized radiation with $T \approx 10^4 \text{ K}$. The dust in the more distant (0.05 pc) second shell absorbs the radiation of the first shell and reradiates it at $T \approx 10^3 \text{ K}$, while simultaneously smoothing out and stretching the light curve. This scenario matches the observed energy, luminosity, time, and temperature scales of the transient by slightly modifying the scenarios used for other hyper-luminous Type II SNe (e.g., Smith et al. 2008a, 2008b; Miller et al. 2010). The host galaxy of the transient is also typical of these SNe, and our estimate of the rate

is consistent with such events being $\sim 10\%$ of hyper-luminous Type II SNe.

The discovery of the progenitors of SN 2008S and NGC300-OT-1 (Prieto et al. 2008; Thompson et al. 2009) as self-observed ($T \sim 400 \text{ K}$, $L \sim 10^5 L_{\odot}$) stars already indicated that mid-IR observations are necessary to understanding the fates of massive stars. If our interpretation of SDWFS-MT-1 is correct, then this may extend to the actual transients as well as to their progenitors, although it is quite likely that SDWFS-MT-1 was also a significant optical transient. IR dust echoes from SNe are relatively common (e.g., Dwek 1983; Rest et al. 2009; Miller et al. 2010), but in these cases the optical depth of the dust is low and the IR emission is only a fraction of what is observed in the optical. A few recent SNe with significant echo luminosities are SN 2007od (Andrews et al. 2010), SN 2006gy (Smith et al. 2007; Miller et al. 2010), SN 2004et (Kotak et al. 2009), and SN 2002hh (Meikle et al. 2006). Obviously, there is a strong selection effect against optically selecting SNe where the optical depth of the surviving dust is near unity, so the true abundance of such sources can only be determined in near/mid-IR searches. There have been some searches made in the near-IR (e.g., Mannucci et al. 2003; Cresci et al. 2007), principally focused on the problem of unassociated foreground absorption rather than dust associated with the progenitor star.

Two important steps are to try and identify massive stars with such dense shells of ejected material, similar to the search for self-observed stars in Thompson et al. (2009) and Khan et al. (2010), and to better characterize the mid-IR emission of other hyper-luminous Type II SNe. If the inner shell invoked to convert the kinetic energy into radiation is dusty, the progenitor will appear as a rapidly cooling near/mid-IR source as the shell expands. Such shells will have temperatures of the order 400 K observed for SN 2008S or NGC300-OT-1 but should show the time variability known to be absent for the SN 2008S progenitor (see Prieto et al. 2008). For the dust to survive the SN explosion and produce a powerful mid-IR transient, it must be considerably more distant and colder than the $T \sim 400 \text{ K}$ dust photosphere of the progenitors of SN 2008S or NGC300-OT-1, with temperatures of order 100 K and SEDs peaking at 20–30 μm that will make them invisible to warm *Spitzer*. In fact, the progenitors may well resemble a moderately colder version of η Carinae, which radiates most of its energy in the mid-IR and has an SED peaking at $\sim 10 \mu\text{m}$ (Robinson et al. 1987). The temperature of such a distant shell will evolve slowly because the timescale for the expansion of the shell is now quite long. Warm *Spitzer* will remain a valuable tool for identifying warm, inner shells, but a careful search for cold outer shells will need to wait for the *James Webb Space Telescope* (JWST).

The *Wide-Field Infrared Survey Explorer* (WISE; Mainzer et al. 2005; Wright et al. 2010), launched in 2009 December, is currently carrying out an all-sky survey at similar wavelengths to *Spitzer*. As a natural by-product of its survey design, it may find many transients similar to SDWFS-MT-1. With a 5σ sensitivity of 0.12 mJy at 3.4 μm and 0.16 mJy at 4.7 μm for a region with eight exposures (Mainzer et al. 2005), WISE has far less sensitivity than the SDWFS survey. Crudely speaking, the survey volume compared to SDWFS scales as the ratio of the (solidangle) (sensitivity) $^{-3/2}$ of the two surveys, so $V_{\text{WISE}}/V_{\text{SDWFS}} \simeq (42000/8)(0.12 \text{ mJy}/6.3 \mu\text{Jy})^{-3/2} \sim 10^2$ and the greater solid angle wins over the reduced sensitivity. If WISE completes two full years of observations, it will also have four epochs, one epoch every 6 months, and so should detect a significant number of these mid-IR transients ($\sim 10^2$).

independent of their origin. For sources closer to the poles of the *WISE* scan pattern, *WISE* will be able to produce detailed light curves. On longer timescales, *JWST* will be able to identify and monitor such luminous transients at almost any redshift.

We thank the anonymous referee, whose comments helped us to improve the manuscript. This work is based on observations made with the *Spitzer Space Telescope*, which is operated by the Jet Propulsion Laboratory (JPL), California Institute of Technology (Caltech) under contract with the National Aeronautics and Space Administration (NASA). Support for this work was provided by NASA through award numbers 1310744 (C.S.K. and S.K.), 1314516 (M.L.N.A.) issued by JPL/Caltech. C.S.K., K.Z.S., T.A.T., and S.K. are also supported by National Science Foundation (NSF) grant AST-0908816. J.L.P. acknowledges support from NASA through Hubble Fellowship grant HF-51261.01-A awarded by STScI, which is operated by AURA, Inc., for NASA, under contract NAS 5-2655. This work made use of images and/or data products provided by NDWFS (Jannuzi & Dey 1999). The NDWFS and the research of A.D. and B.T.J. are supported by the National Optical Astronomy Observatory (NOAO). NOAO is operated by AURA, Inc., under a cooperative agreement with NSF. The CRTS survey is supported by NSF under grants AST-0407448 and AST-0909182. The CSS survey is funded by NASA under grant no. NNG05GF22G issued through the Science Mission Directorate Near-Earth Objects Observations Program.

REFERENCES

- Adelman-McCarthy, J. K., et al. 2006, *ApJS*, **162**, 38
- Andrews, J. E., et al. 2010, *ApJ*, **715**, 541
- Ashby, M. L. N., et al. 2009, *ApJ*, **701**, 428
- Assef, R. J., et al. 2010, *ApJ*, **713**, 970
- Chornock, R., et al. 2010, arXiv:1004.2262
- Cresci, G., Mannucci, F., Della Valle, M., & Maiolino, R. 2007, *A&A*, **462**, 927
- Davidson, K., & Humphreys, R. M. 1997, *ARA&A*, **35**, 1
- Delahaye, F., Pinsonneault, M. H., Pinsonneault, L., & Zeppen, C. J. 2010, arXiv:1005.0423
- Dilday, B., et al. 2010, *ApJ*, **713**, 1026
- Djorgovski, S. G., et al. 2008, *Astron. Nachr.*, **329**, 263
- Draine, B. T. 1981, *ApJ*, **245**, 880
- Drake, A. J., et al. 2009, *ApJ*, **696**, 870
- Drake, A. J., et al. 2010, *ApJ*, **718**, L127
- Dwek, E. 1983, *ApJ*, **274**, 175
- Dwek, E., & Werner, M. W. 1981, *ApJ*, **248**, 138
- Eisenhardt, P. R., et al. 2004, *ApJS*, **154**, 48
- Fazio, G. G., et al. 2004, *ApJS*, **154**, 10
- Gal-Yam, A., et al. 2009, *Nature*, **462**, 624
- Gezari, S., et al. 2009, *ApJ*, **690**, 1313
- Graham, J. R., & Meikle, W. P. S. 1986, *MNRAS*, **221**, 789
- Guhathakurta, P., & Draine, B. T. 1989, *ApJ*, **345**, 230
- Horiuchi, S., Beacom, J. F., & Dwek, E. 2009, *Phys. Rev. D*, **79**, 083013
- Ivezic, Z., & Elitzur, M. 1997, *MNRAS*, **287**, 799
- Izotov, Y. I., Stasińska, G., Meynet, G., Guseva, N. G., & Thuan, T. X. 2006, *A&A*, **448**, 955
- Jannuzi, B. T., & Dey, A. 1999, in ASP Conf. Ser. 191, Photometric Redshifts and the Detection of High Redshift Galaxies, ed. R. Weymann, et al. (San Francisco, CA: ASP), 111
- Karachentsev, I. D. 2005, *AJ*, **129**, 178
- Kewley, L. J., & Ellison, S. L. 2008, *ApJ*, **681**, 1183
- Khan, R., Stanek, K. Z., Prieto, J. L., Kochanek, C. S., Thompson, T. A., & Beacom, J. F. 2010, *ApJ*, **715**, 1094
- Kniazhev, A. Y., Pustilnik, S. A., Grebel, E. K., Lee, H., & Pramskij, A. G. 2004, *ApJS*, **153**, 429
- Kotak, R., et al. 2009, *ApJ*, **704**, 306
- Kozłowski, S., et al. 2010a, *ApJ*, **716**, 530
- Kozłowski, S., Kochanek, C. S., Stern, D., Prieto, J. L., & Stanek, K. Z. 2010b, *CBET*, **2392**, 1
- Krisciunas, K., et al. 2004, *AJ*, **128**, 3034
- Larson, S., Beshore, E., Hill, R., Christensen, E., McLean, D., Kolar, S., McNaught, R., & Garrard, G. 2003, *BAAS*, **35**, 982
- Levesque, E. M., Berger, E., Kewley, L. J., & Bagley, M. M. 2010, *AJ*, **139**, 694
- Loeb, A., & Ulmer, A. 1997, *ApJ*, **489**, 573
- Maguire, K., Kotak, R., Smartt, S. J., Pastorello, A., Hamuy, M., & Bufano, F. 2010, *MNRAS*, **403**, L11
- Mainzer, A. K., Eisenhardt, P., Wright, E. L., Liu, F.-C., Irace, W., Heinrichsen, I., Cutri, R., & Duval, V. 2005, *Proc. SPIE*, **5899**, 262
- Mannucci, F., et al. 2003, *A&A*, **401**, 519
- Meikle, W. P. S., et al. 2006, *ApJ*, **649**, 332
- Miller, A. A., Smith, N., Li, W., Bloom, J. S., Chornock, R., Filippenko, A. V., & Prochaska, J. X. 2010, *AJ*, **139**, 2218
- Miller, A. A., et al. 2009, *ApJ*, **690**, 1303
- Morgan, C. W., Kochanek, C. S., Morgan, N. D., & Falco, E. E. 2010, *ApJ*, **712**, 1129
- Morrissey, P., et al. 2007, *ApJS*, **173**, 682
- Nakar, E. 2007, *Phys. Rep.*, **442**, 166
- Ofek, E. O., et al. 2007, *ApJ*, **659**, L13
- Oke, J. B., et al. 1995, *PASP*, **107**, 375
- Pagel, B. E. J., Edmunds, M. G., Blackwell, D. E., Chun, M. S., & Smith, G. 1979, *MNRAS*, **189**, 95
- Pastorello, A., et al. 2007, *Nature*, **447**, 829
- Peebles, M. S., Pogge, R. W., & Stanek, K. Z. 2008, *ApJ*, **685**, 904
- Pettini, M., & Pagel, B. E. J. 2004, *MNRAS*, **348**, L59
- Pilyugin, L. S., & Thuan, T. X. 2007, *ApJ*, **669**, 299
- Pojmański, G. 1997, *Acta Astron.*, **47**, 467
- Prieto, J. L., Stanek, K. Z., & Beacom, J. F. 2008, *ApJ*, **673**, 999
- Prieto, J. L., et al. 2008, *ApJ*, **681**, L9
- Quimby, R. 2006, *CBET*, **644**, 1
- Quimby, R. M., Aldering, G., Wheeler, J. C., Höflich, P., Akerlof, C. W., & Rykoff, E. S. 2007, *ApJ*, **668**, L99
- Quimby, R., Castro, F., Mondol, P., Caldwell, J., & Terrazas, E. 2007, *CBET*, **793**, 1
- Rest, A., et al. 2009, arXiv:0911.2002
- Robinson, G., Mitchell, R. M., Aitken, D. K., Briggs, G. P., & Roche, P. F. 1987, *MNRAS*, **227**, 535
- Sari, R., Piran, T., & Halpern, J. P. 1999, *ApJ*, **519**, L17
- Schlegel, D. J., Finkbeiner, D. P., & Davis, M. 1998, *ApJ*, **500**, 525
- Seki, J., & Yamamoto, T. 1980, *Ap&SS*, **72**, 79
- Semenov, D., Henning, T., Helling, C., Ilgner, M., & Sedlmayr, E. 2003, *A&A*, **410**, D11
- Skillman, E. D. 1989, *ApJ*, **347**, 883
- Smith, N., Chornock, R., Li, W., Ganeshalingam, M., Silverman, J. M., Foley, R. J., Filippenko, A. V., & Barth, A. J. 2008a, *ApJ*, **686**, 467
- Smith, N., Chornock, R., Silverman, J. M., Filippenko, A. V., & Foley, R. J. 2010, *ApJ*, **709**, 856
- Smith, N., & McCray, R. 2007, *ApJ*, **671**, L17
- Smith, N., & Owocki, S. P. 2006, *ApJ*, **645**, L45
- Smith, N., et al. 2007, *ApJ*, **666**, 1116
- Smith, N., et al. 2008b, *ApJ*, **686**, 485
- Stanek, K. Z., et al. 2006, *Acta Astron.*, **56**, 333
- Starling, R. L. C., et al. 2010, arXiv:1004.2919
- Stern, D., et al. 2005, *ApJ*, **631**, 163
- Terlevich, R., Melnick, J., Masegosa, J., Moles, M., & Copetti, M. V. F. 1991, *A&AS*, **91**, 285
- Thompson, T. A., Prieto, J. L., Stanek, K. Z., Kistler, M. D., Beacom, J. F., & Kochanek, C. S. 2009, *ApJ*, **705**, 1364
- Tremonti, C. A., et al. 2004, *ApJ*, **613**, 898
- van Marle, A. J., Owocki, S. P., & Shaviv, N. J. 2009, *MNRAS*, **394**, 595
- Wambsganss, J. 2006, *Gravitational Lensing: Strong, Weak and Micro*, SAAS-Fee Advanced Courses, Vol. 33 (Berlin: Springer)
- Woolsey, S. E., Blinnikov, S., & Heger, A. 2007, *Nature*, **450**, 390
- Woźniak, P. R., Vestrand, W. T., Panaitescu, A. D., Wren, J. A., Davis, H. R., & White, R. R. 2009, *ApJ*, **691**, 495
- Wright, E. L. 2006, *PASP*, **118**, 1711
- Wright, E. L., et al. 2010, arXiv:1008.0031
- Yin, S. Y., Liang, Y. C., Hammer, F., Brinchmann, J., Zhang, B., Deng, L. C., & Flores, H. 2007, *A&A*, **462**, 535
- Young, D. R., et al. 2010, *A&A*, **512**, A70